2024 IEEE/RSJ International Conference on Intelligent Robots and Systems (IROS)
October 14-18, 2024. Abu Dhabi, UAE

Understanding How a 3-dimensional ZMP Exactly Decouples the Horizontal and Vertical Dynamics of the CoM-ZMP Model

Yuki Onishi[1] and Shuuji Kajita[2]

***Abstract*— The CoM-ZMP model represents the dominant behaviour of bipedal locomotion with surface contact. However, once the centre of mass (CoM) position goes out of a predefined spatial plane, the horizontal dynamics of the model can couple with its vertical dynamics to be nonlinear. This study theoretically investigates the properties of the 3-dimensional zero moment point (ZMP), lying apart from the actual ground to resolve the coupling. The presented discussion includes the compatibility of the 3D ZMP with ZMPs used in preceding research, such as the linear inverted pendulum mode, the existence of a virtual repellent point considering the arbitrary vertical CoM motion, the parameter invariance of the CoM-ZMP model, and feasible regions of the ZMP.**

I. INTRODUCTION

Vertical motion of the centre of mass (CoM) is one of the fundamental components of bipedal locomotion. It naturally appears in everyday behaviour, including walking on slopes and stairs, running, and jumping. Even on flat ground, we can observe that walking with stretched knees and large steps accompanies vertical pelvic motions for both humans [1] and bipedal robots [2], [3], [4]. This observation implies that the vertical CoM motion is not only a characteristic of high-level mobility but also a universal property of bipedal locomotion. Therefore, analysing the vertical CoM motion is a significant milestone in understanding the dynamics of human locomotion and creating advanced bipedal robots. Nevertheless, it is difficult to utilise the vertical CoM motion for bipedal locomotion because of the tight coupling of vertical and horizontal motions. In fact, the CoM dynamics are sometimes modelled as nonlinear forms: e.g., time-variant forms [5], [6], [7] and pure centroidal dynamics [8].

Restricting the vertical motion has strongly supported us deal with the coupling in reduced robot models. Kajita and Tani [9] derived an exactly-linearised reduced system for a planar walking robot by constraining its CoM to lie on a spatial line. The derived system allows us to choose an arbitrary non-vertical line for the CoM path, so their robot succeeded in walking on rugged terrains by switching constraint lines. This model was later extended to a 3-dimensional model [10] and is now widely known as the linear inverted pendulum mode (LIPM), which describes the dominant behaviours of bipedal locomotion with a point mass and a point foot. Pratt and Drakunov [11] extended the LIPM such that the CoM can follow a polynomial curve in the sagittal (x-z) plane. They focused on the concept of orbital energy [12] to design a controller for stable continuous stair walking. Koolen et al. [13] also discussed the orbital energy to achieve bipedal balancing with the vertical CoM motion. They derived a condition for spatially cubic CoM paths such that the orbital energy becomes zero at the origin of a planar LIPM-like model. Their controller automatically lowered the CoM height if the robot lacked its orbital energy, whereas it raised the height in a contrastive case. Ramos and Hauser [14] proposed an algorithm to calculate a capture point [15], [16], a foot position desirable for a robot to balance, for 3-dimensional CoM paths. These studies demonstrated that the vertical CoM motion can improve the balancing ability of biped robots, i.e., capturability [16]. On the other hand, such methods constraining the CoM position still have several issues to apply to a real robot. One of the remarkable issues is the consideration of vertical acceleration limits. While the unilateral condition of contact forces and the CoM height limits were considered in [13] and [14] respectively, a real robot also has joint torque limits that define the feasibility of the CoM acceleration. To investigate this point, Hofslot et al. [17] showed how a capture point changes by vertical motion with acceleration limits. Predefining the CoM paths narrows the class of CoM motions and may limit the performance that can be achieved. Frictional constraints also present another issue.

Instead of the spatial constraints of the CoM, recent results provide another way to resolve the complexity in the CoM dynamics. This direction requires us to reconsider a zero moment point (ZMP): *what and where it is*. Although the ZMP was originally defined as a point on the flat ground [18], it can exist on an certain axis in the 3-dimensional space from its definition, i.e., the ZMP still has one extra degree of freedom [19]. From this perspective, the original ZMP is just an intersection of the axis and flat ground, and it is a special case in which the ZMP is completely equivalent to the centre of pressure (CoP) [20]. The rest degree of freedom enables us to define the ZMP on non-flat ground, e.g., on stairs and rugged terrains [20], [21], [22], [23] (Section II will discuss this topic in detail). Besides, Englsberger et al. [24] pointed out that there exists the enhanced centroidal moment pivot (eCMP), a generalisation of the ZMP accepting tilting

*This work was supported by JSPS KAKENHI (Grant Number: JP20H02124 and JP23KJ0889) and Japan Science and Technology Agency, ACT-X (Grant Number: JPMJAX2008).

[1]Yuki Onishi is with the Department of Systems and Control Engineering, School of Engineering, Tokyo Institute of Technology, 2-12-1 Ookayama, Meguro, Tokyo 152-8550, Japan. He is also appointed as a research fellow of Japan Society for the Promotion of Science, Japan. onishi@sl.sc.e.titech.ac.jp

[2]Shuuji Kajita is with the Department of Artificial Intelligence and Robotics, College of Science and Engineering, Chubu University, 1200 Matsumoto-cho, Kasugai, Aichi 487-8501, Japan. shuuji.kajita@fsc.chubu.ac.jp

moments around the CoM. The eCMP is defined such that the CoM dynamics are represented by a linear system. Inheriting these mathematical results, Sugihara et al. [25] recently proposed the concept of a 3-dimensional ZMP. They considered a ZMP apart from the ground to represent arbitrary CoM motions, including jumping and running, as a linear system in a unified manner. Such a representation has the potential to develop a new theory of bipedal locomotion with exact linearity, but the effects of ZMP height variation are still unclear.

The contribution of this paper is to reveal how the 3-dimensional ZMP encodes the interference of the vertical CoM motion in the horizontal dynamics while conserving the model linearity. Furthermore, this paper also shows some properties of the 3-dimensional ZMP through reviews and generalisation of preceding research.

II. PRELIMINARIES

A. Zero Moment Point

This subsection briefly reviews the definition of the ZMP, following the discussion in [19]. Let $\boldsymbol{p}_G = [x_G,\ y_G,\ z_G]^\mathsf{T} \in \mathbb{R}^3$ and $\boldsymbol{h}_G \in \mathbb{R}^3$ be the CoM position and angular momentum around the CoM of the biped robot, respectively. We can then describe the equations of motion (EoMs) of the CoM, also known as centroidal dynamics:

$$m\ddot{\boldsymbol{p}}_G = \boldsymbol{f} - m\boldsymbol{g}, \tag{1a}$$

$$\dot{\boldsymbol{h}}_G = -(\boldsymbol{p}_G - \boldsymbol{p}_X) \times \boldsymbol{f} + \boldsymbol{\tau}_X. \tag{1b}$$

Here, $m > 0$ is the total mass, and $\boldsymbol{g} = [0,\ 0,\ g]^\mathsf{T} \in \mathbb{R}^3$ is the gravitational vector with the gravitational acceleration constant g. The former equation (1a) is Newton's EoM representing the translational motion of the CoM, whereas the latter (1b) is Euler's EoM for rotational motion around a certain point $\boldsymbol{p}_X \in \mathbb{R}^3$. The two vectors $\boldsymbol{f},\ \boldsymbol{\tau}_X \in \mathbb{R}^3$ denote the total external force and torque around $\boldsymbol{p}_X$ acting from the environment to the robot, respectively.

The point $\boldsymbol{p}_X$ becomes a zero moment point (ZMP) when the horizontal momenta around the point $\boldsymbol{p}_X$ balance. Formally, the ZMP is a point satisfying the following equation:

$$\boldsymbol{g} \times \boldsymbol{\tau}_X = \boldsymbol{0} \quad \left(\Leftrightarrow\ \boldsymbol{\tau}_X = \begin{bmatrix} 0 & 0 & * \end{bmatrix}^\mathsf{T}\right). \tag{2}$$

From the EoMs (1), we can rewrite (2) into

$$\boldsymbol{g} \times \left\{(\boldsymbol{p}_G - \boldsymbol{p}_X) \times m(\ddot{\boldsymbol{p}}_G + \boldsymbol{g}) + \dot{\boldsymbol{h}}_G\right\} = \boldsymbol{0}. \tag{3}$$

Let us define a ZMP with this equation.

Definition 1 (ZMP): A point $\boldsymbol{p}_X$ is a ZMP if and only if $\boldsymbol{p}_X$ satisfies (3).

Transforming (3) with elemental expressions $\boldsymbol{p}_X = [x_X,\ y_X,\ z_X]^\mathsf{T}$ and $\boldsymbol{h}_G = [h_{G,x},\ h_{G,y},\ h_{G,z}]^\mathsf{T}$, we obtain

$$\begin{cases} (x_G - x_X)(\ddot{z}_G + g) = \ddot{x}_G(z_G - z_X) + \dfrac{\dot{h}_{G,y}}{m} \\ (y_G - y_X)(\ddot{z}_G + g) = \ddot{y}_G(z_G - z_X) - \dfrac{\dot{h}_{G,x}}{m} \end{cases}. \tag{4}$$

While the ZMP is defined in a 3-dimensional space, the definition has only two scalar equations. For this reason, the ZMP has a 1-dimensional expanse (one degree of freedom), despite the "point" in the name. We will discuss this property with a specified model in the upcoming subsection II-C.

B. From Centroidal Dynamics to the CoM-ZMP Model

Given a ZMP $\boldsymbol{p}_Z = [x_Z,\ y_Z,\ z_Z]^\mathsf{T} \in \mathbb{R}^3$, we can rewrite the centroidal dynamics of a biped robot (1) as

$$m\ddot{\boldsymbol{p}}_G = \boldsymbol{f} - m\boldsymbol{g}, \tag{5a}$$

$$\dot{\boldsymbol{h}}_G = -(\boldsymbol{p}_G - \boldsymbol{p}_Z) \times \boldsymbol{f} + \boldsymbol{\tau}_Z. \tag{5b}$$

Suppose that $\boldsymbol{g} \times \dot{\boldsymbol{h}}_G \simeq \boldsymbol{0}$, namely, the momentum rates around the horizontal (x- and y-) axes are sufficiently small. Then, we can derive the following equation using both the centroidal EoMs (5) and the ZMP condition $\boldsymbol{g} \times \boldsymbol{\tau}_Z = \boldsymbol{0}$:

$$\begin{aligned} \boldsymbol{g} \times \dot{\boldsymbol{h}}_G &= \boldsymbol{g} \times \{-(\boldsymbol{p}_G - \boldsymbol{p}_Z) \times \boldsymbol{f}\} \\ &= \boldsymbol{g} \times \{-(\boldsymbol{p}_G - \boldsymbol{p}_Z) \times m(\ddot{\boldsymbol{p}}_G + \boldsymbol{g})\} = \boldsymbol{0} \end{aligned} \tag{6}$$

$$\Leftrightarrow\ \boldsymbol{g} \times \{(\boldsymbol{p}_G - \boldsymbol{p}_Z) \times (\ddot{\boldsymbol{p}}_G + \boldsymbol{g})\} = \boldsymbol{0}. \tag{7}$$

The third-elemental equation of (7) is an identity, thus it provides no information. Since the first and second elements of the vector $\boldsymbol{g}$ are zero, (7) holds regardless of the third (z-) element of the cross product $(\boldsymbol{p}_G - \boldsymbol{p}_Z) \times (\ddot{\boldsymbol{p}}_G + \boldsymbol{g})$. In contrast, the first and second elements of $(\boldsymbol{p}_G - \boldsymbol{p}_Z) \times (\ddot{\boldsymbol{p}}_G + \boldsymbol{g})$ must be zero to satisfy (7) since the third element of $\boldsymbol{g}$ is the constant g. For these reasons, the condition (7) is essentially equivalent to

$$\begin{cases} (y_G - y_Z)(\ddot{z}_G + g) = \ddot{y}_G(z_G - z_Z) \\ (x_G - x_Z)(\ddot{z}_G + g) = \ddot{x}_G(z_G - z_Z) \end{cases}. \tag{8}$$

Assume a situation in which the total external force applies to the robot at a point lower than the CoM position, then an inequality $\boldsymbol{g}^\mathsf{T}(\boldsymbol{p}_G - \boldsymbol{p}_Z) > 0\ \ (\Rightarrow z_G - z_Z > 0)$ holds. This is because the ZMP $\boldsymbol{p}_Z$ acts as an equivalent point of application of the total external force $\boldsymbol{f}$. Now introducing a system parameter ω as

$$\omega = \sqrt{\frac{\ddot{z}_G + g}{z_G - z_Z}}, \tag{9}$$

we can obtain one EoM of the CoM that satisfies (8):

$$\ddot{\boldsymbol{p}}_G + \boldsymbol{g} = \omega^2(\boldsymbol{p}_G - \boldsymbol{p}_Z). \tag{10}$$

This EoM is called the CoM-ZMP model if we regard the ZMP $\boldsymbol{p}_Z$ as a control input [26]. Note that the third row of this vector equation is identical and that ω is not limited to a constant at this time.

C. The extra degree of freedom of ZMP

As we found in II-A, the definition of the ZMP constrains only two degrees of freedom, whereas the ZMP is a point in the 3-dimensional space. Thus, points satisfying the ZMP definition (3) distribute with a 1-dimensional expanse in the 3-dimensional space. This fact was pointed out by Sardain and Bessonnet [19] and Popovic et al. [20]. Originally, Vukobratović and Stepanenko [18] introduced the ZMP as a point on the flat ground where horizontal (tilting) momenta

balance. However, later analysis clarified that the point is just an intersection of the flat ground and the set of points. It was also shown that the original ZMP and centre of pressure (CoP) [27] coincide only on the flat ground [19]. We can find pioneering challenges in treating a ZMP apart from the ground before those theoretical advancement: Kagami et al. [21] considered a ZMP for a humanoid robot with non-coplanar contacts, and Sugihara et al. [22] did it for a biped locomotion on uneven terrains. Caron et al. [23] provided detailed summary of these results and generalised formulation of the ZMP, including consideration of frictional constraints.

In the CoM-ZMP model, the ZMP lies on a line passing through the CoM position, and the following lemma holds.

Lemma 1: Consider the CoM-ZMP model (10). When a point $\boldsymbol{p}_Z$ satisfying (3) is given, any point on a line through the CoM position $\boldsymbol{p}_G$ and $\boldsymbol{p}_Z$ also satisfies (3).

Proof: We can describe any point on a line through $\boldsymbol{p}_G$ and $\boldsymbol{p}_Z$ as $\boldsymbol{p}'_Z = \alpha\boldsymbol{p}_G + (1-\alpha)\boldsymbol{p}_Z$ with a scalar $\alpha \in \mathbb{R}$. Under the assumption $\boldsymbol{g} \times \dot{\boldsymbol{h}}_G = 0$, a substitution $\boldsymbol{p}_X = \boldsymbol{p}'_Z$ in the left side of the ZMP condition (3) yields

$$\begin{aligned} &\boldsymbol{g} \times \{(1-\alpha)\,(\boldsymbol{p}_G - \boldsymbol{p}_Z) \times m\,(\ddot{\boldsymbol{p}}_G + \boldsymbol{g})\} \\ &= (1-\alpha) \cdot \boldsymbol{g} \times \{(\boldsymbol{p}_G - \boldsymbol{p}_Z) \times m\,(\ddot{\boldsymbol{p}}_G + \boldsymbol{g})\} = \boldsymbol{0}, \end{aligned} \tag{11}$$

as $\boldsymbol{p}_Z$ satisfies (3). ■

III. 3-DIMENSIONAL ZMP

The tight coupling of the horizontal and vertical CoM motion lies in the CoM-ZMP model (10) via the variable parameter ω. This section resolves the coupling with a choice of the ZMP.

A. ZMP Height Variation for the Vertical CoM Motion

The system parameter ω depends on the CoM height z_G, the vertical CoM acceleration $\ddot{z}_G$, and the ZMP height z_Z, as defined in (9). Using the methods proposed by Kajita et al. [9], [10], we can make ω constant by constraining the CoM position on a spatial plane. However, such a constraint determines not only the CoM height z_G but also the vertical CoM acceleration $\ddot{z}_G$ because of the geometrical relationship.

In contrast, Sugihara et al. [25] proposed to vary the ZMP height z_Z. If we allow a ZMP to exist apart from the actual ground, nothing constrains its height. As discussed in II-C, candidates of the ZMP are found on a spatial line, so we can choose one from the line as we desire. Let us choose a ZMP suitable for treating the vertical CoM motion so that its height satisfies the following relationship with a nominal constant parameter $\omega_0 > 0$:

$$z_Z = z_G - \frac{1}{\omega_0^2}\,(\ddot{z}_G + g)\,. \tag{12}$$

To distinguish it from conventional ZMPs fixed on the ground, we call a ZMP with this height a 3-dimensional ZMP.

Definition 2 (3-dimensional ZMP): A ZMP is called 3-dimensional ZMP (3D ZMP) if and only if its height is determined by (12).

The 3D ZMP completely decouples the horizontal and vertical CoM dynamics of the CoM-ZMP model. Substituting the ZMP height (12) into the definition of ω (9), we can make the parameter ω constant, namely, $\omega = \omega_0$.

Theorem 1 ([25]): With the 3D ZMP, the CoM dynamics (10) become exactly affine:

$$\ddot{\boldsymbol{p}}_G + \boldsymbol{g} = \omega_0^2\,(\boldsymbol{p}_G - \boldsymbol{p}_Z)\,. \tag{13}$$

The 3D ZMP height (12) *superficially* absorbs the effects from vertical motion to horizontal motion; thus, (13) can describe the arbitrary motion of the CoM with an affine expression. On the other hand, the effects actually work: this is why the word "superficially" is used here. Sction IV-B explains how these effects appear in the model.

The transformation of the CoM dynamics (13) yields a generalised form of the ZMP equation [28], which calculates the ZMP from the CoM position and acceleration.

$$\boldsymbol{p}_Z = \boldsymbol{p}_G - \frac{1}{\omega_0^2}\,(\ddot{\boldsymbol{p}}_G + \boldsymbol{g})\,. \tag{14}$$

Note that a ZMP provided by the ZMP equation (14) can differ from an actual 3D ZMP under disturbances.

Let $h = g/\omega_0^2 \ \left(\Leftrightarrow \omega_0 = \sqrt{g/h}\right)$ be the nominal CoM height on flat ground. Then, the following situations help us to understand how the 3D ZMP behaves.

- When the CoM height moves on a horizontal plane with a nominal height h, the 3D ZMP height becomes 0. If the ground is flat and is represented by $z = 0$, the 3D ZMP lies on the ground.
- When the CoM height moves on a plane with a constant height $h \pm \delta$, the 3D ZMP height becomes $\pm\delta$. The height changes to compensate for the error in the CoM height from the nominal value.
- When the CoM accelerates upward/downward from the initial height h, the 3D ZMP sinks/floats, respectively. Generating the vertical acceleration is momentarily equivalent to changing the magnitude of gravity. Therefore, the 3D ZMP moves to build a *virtual CoM-ZMP model* that has the same parameter ω_0 in a different gravitational field.

The last case provides the essence of the proposed formulation, i.e., the construction of a virtual CoM-ZMP model. To conserve the horizontal linearity with the constant ω_0, the model must always cancel the coupling effect of the vertical motion by modifying the ZMP position. The modification may construct a different CoM-ZMP model depending on the vertical CoM position and acceleration at each time, but all of them hold the *dynamical similarity* with respect to the horizontal dynamics. Altogether, the 3D ZMP moves to exhibit this dynamical similarity.

B. Virtual Repellent Point

While this study treats the vertical CoM motion of a biped robot in a linear representation, Englsberger et al. [24] addressed a similar problem with nonzero angular momenta around the CoM. Although their theory cannot deal with the arbitrary vertical motion of the CoM, they provided insightful

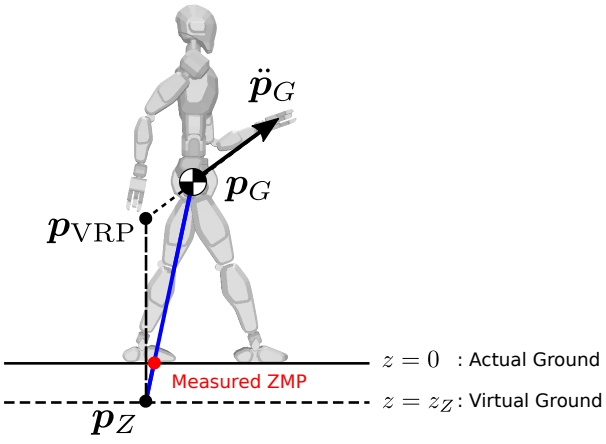

Fig. 1. The geometrical relationship of the 3D ZMP, the VRP, and the measured ZMP on the flat ground

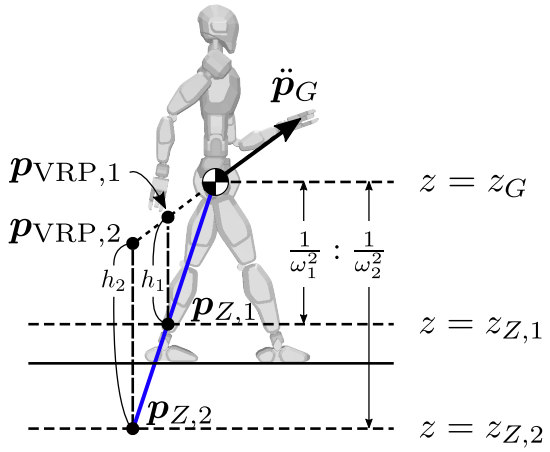

Fig. 2. The relationship of two 3D ZMPs and two VRPs with two different nominal parameters, ω_1 and ω_2. Here, $h_1 = g/\omega_1^2$ and $h_2 = g/\omega_2^2$

results and discussions that strongly inspired this research. One of them is the introduction of a virtual repellent point (VRP), which works as a repeller of the CoM motion. The following discussion will show that there also exists a VRP that can consider the arbitrary vertical motion of the CoM.

Definition 3 (Virtual repellent point): For a 3D ZMP $\boldsymbol{p}_Z$, a VRP is defined by

$$\boldsymbol{p}_{\mathrm{VRP}} = \boldsymbol{p}_Z + \begin{bmatrix} 0 & 0 & h \end{bmatrix}^{\mathsf{T}}, \tag{15}$$

where $h = g/\omega_0^2$ denotes the nominal height of the CoM.

Theorem 2: Using the VRP, we can write the EoM of the CoM as a simple representation, where the CoM looks just repelled by the VRP (see Fig. 1):

$$\ddot{\boldsymbol{p}}_G = \omega_0^2 \left(\boldsymbol{p}_G - \boldsymbol{p}_{\mathrm{VRP}}\right) \tag{16}$$

Proof: Substituting (15) into the CoM-ZMP model (13) yields (16). The vertical offset with h in the VRP definition (15) cancels the gravitational term in (13). ■

C. Parameter invariance

Both the EoM with the 3D ZMP (13) and the derived representation (16) include the designable parameter $\omega_0 > 0$. However, even if we choose any parameter $\omega_0 > 0$, the described CoM motion is unique and invariant. Let us check this fact.

Theorem 3: The EoM of the CoM with the 3D ZMP (13) is invariant with respect to the nominal parameter $\omega_0 > 0$.

Proof: We demonstrate that two EoMs with different parameters represent the same CoM motion. Consider two parameters, ω_1 and ω_2 satisfying $\omega_1 > \omega_2 > 0$. Using the 3D ZMPs, we obtain two EoMs for the horizontal CoM motion.

$$\ddot{\boldsymbol{p}}_G + \boldsymbol{g} = \omega_1^2 \left(\boldsymbol{p}_G - \boldsymbol{p}_{Z,1}\right), \tag{17a}$$
$$\ddot{\boldsymbol{p}}_G + \boldsymbol{g} = \omega_2^2 \left(\boldsymbol{p}_G - \boldsymbol{p}_{Z,2}\right). \tag{17b}$$

Here, we describe the 3D ZMPs corresponding to ω_1 and ω_2 with $\boldsymbol{p}_{Z,1}$ and $\boldsymbol{p}_{Z,2}$, respectively.

Remind that the nominal parameters are not only the coefficients of the CoM dynamics but also determine the ZMP heights through (12):

$$z_{Z,1} = z_G - \frac{1}{\omega_1^2}\left(\ddot{z}_G + g\right), \tag{18a}$$
$$z_{Z,2} = z_G - \frac{1}{\omega_2^2}\left(\ddot{z}_G + g\right). \tag{18b}$$

For these ZMP heights and Lemma 1, the following geometrical relationship holds (Fig. 2).

$$\boldsymbol{p}_G - \boldsymbol{p}_{Z,1} = \frac{\omega_2^2}{\omega_1^2}\left(\boldsymbol{p}_G - \boldsymbol{p}_{Z,2}\right). \tag{19}$$

This is the scaling of ZMP relative to the CoM. In other words, this equation projects the 3D ZMP $\boldsymbol{p}_{Z,2}$ corresponding to ω_2 onto the virtual plane whose height is determined by ω_1, satisfying the dynamical constraints. A substitution of this equation into (17a) yields

$$\ddot{\boldsymbol{p}}_G + \boldsymbol{g} = \omega_1^2 \cdot \frac{\omega_2^2}{\omega_1^2}\left(\boldsymbol{p}_G - \boldsymbol{p}_{Z,2}\right) = \omega_2^2 \left(\boldsymbol{p}_G - \boldsymbol{p}_{Z,2}\right), \tag{20}$$

namely, the other EoM (17b). Two EoMs with different parameters (17a) and (17b) completely matches by the geometrical relationship of the 3D ZMPs. ■

Some readers may concern that the choice of this parameter is important to describe the CoM motion in system modelling. In fact, many preceding papers think that varying the nominal parameter ω_0 changes the system behaviours with formulation in which the ZMP lies on the ground: the parameter defines the convergence and divergence components of motion (CCM and DCM) [29] and affects the capturability analysis [11], [16]. The work by Englsberger et al. [24], in which we share the basic direction of research, also regarded a nominal height h, which determines the nominal parameter $\omega_0 = \sqrt{g/h}$ in the paper, as a designable variable while considering variable angular momentum. However, Theorem 3 reveals that any nominal parameter derives the same CoM dynamics in the formulation using the ZMP height (12). Since the original CoM dynamics are unique, this parameter invariance would be a natural property.

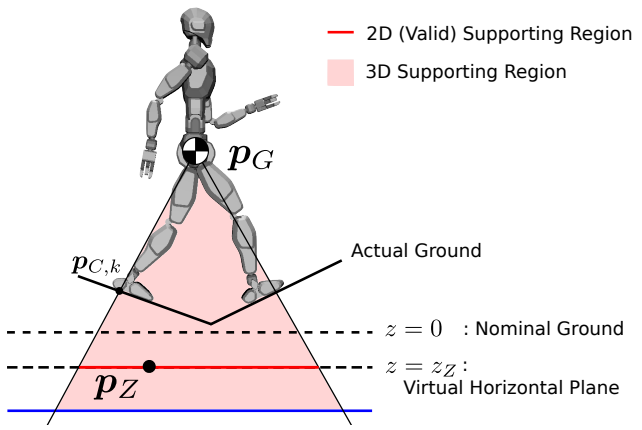

Fig. 3. The 3D supporting region. It forms a convex cone whose origin is the CoM. Its boundaries include all the contact points. A section of this region with any virtual horizontal plane with a given ZMP height corresponds to the 2D supporting polygon (red line). If the vertical CoM acceleration is limited, the 3D support region has the bottom (blue line) and forms a polyhedron.

D. Compatibility of the 3D ZMP with a Measured ZMP

Historically, biped robots have measured the ZMP with pressure sensors and force/torque (F/T) sensors. The measured ZMP basically lies on a predefined plane, e.g., the flat ground. The compatibility of the 3D ZMP with the measured ZMPs can be explained as follows.

Following the discussion in II-C, a point satisfying the ZMP definition can exist anywhere on one spatial line passing through the CoM. Once one point is given, we can determine the line by connecting the point with the CoM from Lemma 1. Therefore, when a robot measures a ZMP on a certain plane with sensors, the 3D ZMP exists on the line through the CoM and the measured ZMP, and vice versa. Fig. 1 illustrates this relationship. The line is generally non-vertical, so the horizontal elements of the 3D ZMP and the measured ZMP do not match.

IV. The 3-dimensional Support Region

We can generalise a support region, also known as a support polygon, for the 3D ZMP, as pointed out in [25]. The generalised support region forms a convex cone whose origin is the CoM position:

$$\mathcal{S}_Z = \left\{ \boldsymbol{p}_Z \,\middle|\, \boldsymbol{p}_Z = \boldsymbol{p}_G + \sum_{k=1}^{N} \alpha_k \left(\boldsymbol{p}_{C,k} - \boldsymbol{p}_G \right),\ \forall \alpha_k \geq 0 \right\}, \tag{21}$$

where $\boldsymbol{p}_{C,k}$ is the k-th contact point between the robot and environment, and N represents the number of contact points. Fig. 3 illustrates this region. This region includes the surfaces of the cone, which correspond to the edges of the 2D support region. Although we do not consider the line and surface contact conditions which yield an infinite number of contact points, sampling representative contact points is expected to work well.

On the flat ground, this 3-dimensional formulation (21) completely covers the support polygon [30]. In this case, the intersection of the 3D support region and flat ground forms a convex hull of all contact points. In addition, it also covers the 2D support region on uneven terrains presented in [22], where the concept of the virtual horizontal plane firstly appeared.

A. Vertical Acceleration Limits of the CoM

A real robot has limitations in its vertical acceleration of the CoM. The lower limit of the vertical CoM acceleration is trivially $-g$, as observed in a free-fall motion. This is because of the unilateral conditions of the contact forces. In this case, from (12), the ZMP height becomes equivalent to the CoM height $z_Z = z_G$, and the support region (21) degenerates into only one point $\boldsymbol{p}_G$ [25].

On the other hand, the upper limit is determined by joint effort limits and kinematic structures. Simply given the upper limit $\ddot{z}_{G,\max}$, we can calculate the lower limit of the ZMP height as

$$z_Z = z_G - \frac{1}{\omega_0^2} \left(\ddot{z}_{G,\max} + g \right). \tag{22}$$

Consequently, in real applications, the 3D support region has the lower bound and forms a polyhedron as shown in Fig. 3.

B. Scaling of 2D Support Region

As the preceding paper [31] pointed out, the stabilisable region of the CoM-ZMP model with surface contacts, where a robot can balance without stepping, is determined by the horizontal ZMP limits and the system parameter ω by (9). Without loss of generality, let us focus on the dynamics along the x-axis as one horizontal direction. The state equation of the x-dynamics using the fixed ZMP height $z_Z = 0$ and the variable parameter ω is

$$\frac{d}{dt} \begin{bmatrix} x_G \\ \dot{x}_G \end{bmatrix} = \begin{bmatrix} 0 & 1 \\ \omega^2 & 0 \end{bmatrix} \begin{bmatrix} x_G \\ \dot{x}_G \end{bmatrix} + \begin{bmatrix} 0 \\ -\omega^2 \end{bmatrix} x_Z. \tag{23}$$

Without CoM vertical motion, the stabilisable region is the area between the following two straight lines [31]:

$$x_G + \frac{1}{\omega} \dot{x}_G = x_{Z,\min}, \tag{24a}$$

$$x_G + \frac{1}{\omega} \dot{x}_G = x_{Z,\max}, \tag{24b}$$

where $x_{Z,\min}$ and $x_{Z,\max}$ are the limits of 2D support region, i.e., $x_Z \in [x_{Z,\min}, x_{Z,\max}]$. Fig. 4 draws these lines on the phase portrait in blue. With the best CoM-ZMP regulator [31], which is now also known as the DCM feedback controller, the CoM asymptotically converges to the origin (or a reference CoM state) if the initial state lies inside the stabilisable region.

In (24), the ZMP limits and the parameter ω correspond to the horizontal intercepts and slope magnitude of the boundary lines, respectively. As the ZMP limits depend on the contact states, ω is only one parameter that modifies the region without stepping. Varying ω yields rotations of the boundaries around each intercept. If $x_{Z,\min} < x_G < x_{Z,\max}$, then increasing ω can be regarded as a local expansion of

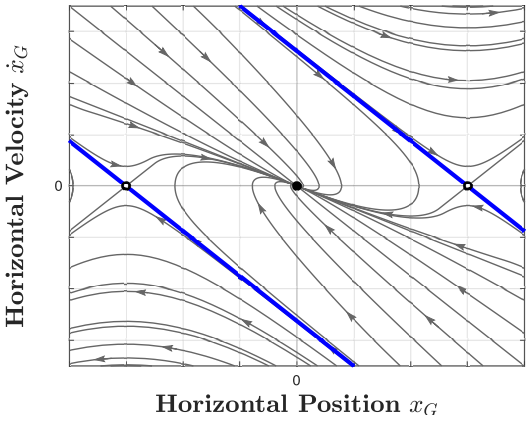

Fig. 4. A phase portrait of the x-directional CoM dynamics applied the best CoM-ZMP regulator (a.k.a. DCM feedback controller). With the controller, the stabilisable region bounded by the blue lines (24) matches the stable region. Thus, all states inside the bounded region converge asymptotically into the origin (black point) under regulation. The boundaries have the same slope $-\omega$. The intersection between the stabilisable region and the x axis corresponds to the 2D support region.

the stable region. Utilising this property, Yamamoto et al. [7] proposed a time-variant controller that modulates ω with the vertical CoM motion for bipedal balancing.

Instead of the variation of ω, in the formulation with the 3D ZMP, the 2D support region scales according to the 3D ZMP height, which encodes the vertical CoM position and acceleration. Let us check that we can explain the change of stabilisable boundaries even with the constant parameter ω_0 through an example. Once vertical motion occurs with the initial CoM height $h = g/\omega_0^2$, the ZMP also moves vertically, and the limits of the 2D support region $\left[x'_{Z,\min},\ x'_{Z,\max}\right]$ is scaled by the following geometrical relationship.

$$\begin{aligned} x'_Z &= \frac{h - z_Z}{h}\left(x_Z - x_G\right) + x_G \\ &= \frac{h - z_Z}{h}x_Z + \frac{z_Z}{h}x_G = \frac{g + \ddot{z}_G}{g}x_Z + \frac{\ddot{z}_G}{g}x_G \end{aligned} \tag{25}$$

Here, we use the initial condition $z_G = h$. The following state equation represents the horizontal dynamics:

$$\begin{aligned} \frac{d}{dt}\begin{bmatrix} x_G \\ \dot{x}_G \end{bmatrix} &= \begin{bmatrix} 0 & 1 \\ \omega_0^2 & 0 \end{bmatrix}\begin{bmatrix} x_G \\ \dot{x}_G \end{bmatrix} + \begin{bmatrix} 0 \\ -\omega_0^2 \end{bmatrix} x'_Z \\ &= \begin{bmatrix} 0 & 1 \\ \frac{\ddot{z}_G + g}{g}\cdot\omega_0^2 & 0 \end{bmatrix}\begin{bmatrix} x_G \\ \dot{x}_G \end{bmatrix} + \begin{bmatrix} 0 \\ -\frac{\ddot{z}_G + g}{g}\cdot\omega_0^2 \end{bmatrix} x_Z \end{aligned} \tag{26}$$

Focusing on the coefficient matrix, we find that the eigenvalues vary from $\pm\omega_0$ to $\pm\sqrt{\left(\ddot{z}_G + g\right)/g}\cdot\omega_0$. Therefore, with the constant parameter ω_0, the boundaries are represented by

$$x_G + \sqrt{\frac{g}{\ddot{z}_G + g}}\cdot\frac{1}{\omega_0}\dot{x}_G = x_{Z,\min}, \tag{27a}$$

$$x_G + \sqrt{\frac{g}{\ddot{z}_G + g}}\cdot\frac{1}{\omega_0}\dot{x}_G = x_{Z,\max}. \tag{27b}$$

For the definition of the variable parameter ω (9),

$$\omega = \sqrt{\frac{\ddot{z}_G + g}{h}} = \sqrt{\frac{\ddot{z}_G + g}{g}}\omega_0. \tag{28}$$

Hence, the boundaries with the constant parameter ω_0 (27) completely match the boundaries with the variable ω (24). Fig. 5 illustrates this relationship on the phase portrait.

This discussion has no loss of generality, and we can apply the results to all horizontal directions. While the variation of ω describes the change of the stabilisable region with ZMPs on the ground, the scale of the 2D support region explains the same phenomenon.

V. SUMMARY

This paper investigated how the 3D ZMP behaves for arbitrary CoM motions. The key points are summarised as follows:

1) The 3D ZMP varies its height to represent the vertical CoM motion while keeping the affinity of the CoM-ZMP model and the linearity of the CoM-VRP model.
2) The 3D support region encodes the interference between the vertical and horizontal dynamics as local scaling of 2D support region.

In addition, this paper reveals not only the exact model linearity but also the invariance of ω_0 and the existence of the virtual repellent point even with arbitrary vertical CoM motions. Future work includes controller design using these properties effectively for various types of bipedal locomotion. The discussed model is expected to reduce computational costs of planning and control.

ACKNOWLEDGMENT

The authors would like to thank Prof. Mitsuji Sampei at Tokyo Institute of Technology for giving Yuki Onishi an opportunity to work in Chubu University. The authors are also grateful to Dr. Tomomichi Sugihara at OMRON Corp. for having deep discussion on the 3D ZMP manipulation [25].

REFERENCES

[1] J. Rose, *Human walking / edited by Jessica Rose and James G. Gamble.*, 3rd ed. Philadelphia, Penn. ; London: Lippincott Williams & Wilkins, 2006.

[2] Y. Ogura, K. Shimomura, H. Kondo, A. Morishima, T. Okubo, S. Momoki, H. Lim, and A. Takanishi, "Human-like walking with knee stretched, heel-contact and toe-off motion by a humanoid robot," in *Proceedings of 2006 IEEE/RSJ International Conference on Intelligent Robots and Systems*, 2006, pp. 3976–3981.

[3] R. J. Griffin, G. Wiedebach, S. Bertrand, A. Leonessa, and J. Pratt, "Straight-leg walking through underconstrained whole-body control," in *Proceedings of 2018 IEEE International Conference on Robotics and Automation*, 2018, pp. 5747–5754.

[4] Y. Onishi, S. Kajita, T. Ibuki, and M. Sampei, "Knee-stretched biped gait generation along spatially quantized curves," in *Proceedings of 2021 IEEE/RSJ International Conference on Intelligent Robots and Systems*, 2021, pp. 5120–5127.

[5] M. A. Hopkins, D. W. Hong, and A. Leonessa, "Humanoid locomotion on uneven terrain using the time-varying divergent component of motion," in *Proceedings of 2014 IEEE-RAS International Conference on Humanoid Robots*, 2014, pp. 266–272.

[6] S. Caron, A. Escande, L. Lanari, and B. Mallein, "Capturability-based pattern generation for walking with variable height," *IEEE Transactions on Robotics*, vol. 36, no. 2, pp. 517–536, 2020.

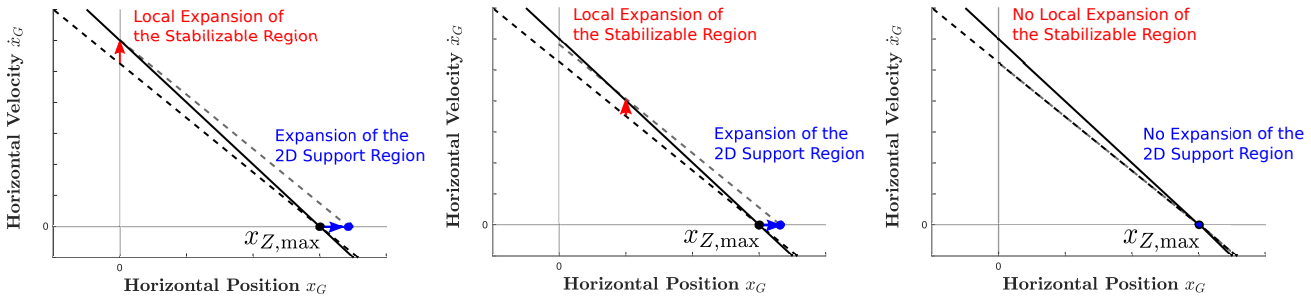

(a) For $x_G = 0$ (b) For $x_G = x_{Z,\max}/3$ (c) For $x_G = x_{Z,\max}$

Fig. 5. The first quadrant of the phase portrait of the x-directional CoM dynamics. The dotted black lines represent the boundary when $\omega = \omega_0$. In formulations in whih the ZMP height is kept constant, if positive vertical CoM acceleration $\ddot{z}_G = a$ occurs, it increases the value of ω such that the boundary rotates clockwise around $\left[x_{Z,\max},\ 0\right]$, as indicated by the black non-dotted lines. Thus, the stabilisable region expands locally when the CoM position x_G lies inside the nominal 2D support region $\left[x'_{Z,\min},\ x'_{Z,\max}\right]$. The red arrows in (a) and (b) indicate this local expansion for $x_G = 0$ and $x_G = x_{Z,\max}/3$, respectively. By contrast, in the formulation with the 3D ZMP, the maximum 2D support limit expands from $x_{Z,\max}$ to $\frac{a+g}{g} \cdot x_{Z,\max}$ following (25) (blue arrows in (a) and (b)). This expansion of the 2D support region yields parallel movements from the black dotted lines to the dotted gray lines, which work equivalently to the aforementioned rotation. Note that the magnitude of parallel movements strongly depends on the CoM position relative to the 2D support limits. Especially, no movement appears when $x_G = x_{Z,\max}$ as shown in (c).

[7] K. Yamamoto, N. Kobayashi, T. Ishigaki, and Y. Sakemi, "Integration of variable-height and hopping strategies for humanoid push recovery," in *Proceedings of 2022 IEEE/RSJ International Conference on Intelligent Robots and Systems*, 2022, pp. 12 979–12 985.

[8] H. Dai, A. Valenzuela, and R. Tedrake, "Whole-body motion planning with centroidal dynamics and full kinematics," in *Proceedings of 2014 IEEE-RAS International Conference on Humanoid Robots*, 2014, pp. 295–302.

[9] S. Kajita and K. Tani, "Study of dynamic biped locomotion on rugged terrain-derivation and application of the linear inverted pendulum mode," in *Proceedings of 1991 IEEE International Conference on Robotics and Automation*, vol. 2, 1991, pp. 1405–1411.

[10] S. Kajita, F. Kanehiro, K. Kaneko, K. Yokoi, and H. Hirukawa, "The 3d linear inverted pendulum mode: a simple modeling for a biped walking pattern generation," in *Proceedings of 2001 IEEE/RSJ International Conference on Intelligent Robots and Systems*, vol. 1, 2001, pp. 239–246.

[11] J. E. Pratt and S. V. Drakunov, "Derivation and application of a conserved orbital energy for the inverted pendulum bipedal walking model," in *Proceedings of 2007 IEEE International Conference on Robotics and Automation*, 2007, pp. 4653–4660.

[12] S. Kajita, T. Yamaura, and A. Kobayashi, "Dynamic walking control of a biped robot along a potential energy conserving orbit," *IEEE Transactions on Robotics and Automation*, vol. 8, no. 4, pp. 431–438, 1992.

[13] T. Koolen, M. Posa, and R. Tedrake, "Balance control using center of mass height variation: Limitations imposed by unilateral contact," in *Proceedings of 2016 IEEE-RAS International Conference on Humanoid Robots*, 2016, pp. 8–15.

[14] O. E. Ramos and K. Hauser, "Generalizations of the capture point to nonlinear center of mass paths and uneven terrain," in *Proceedings of 2015 IEEE-RAS International Conference on Humanoid Robots*, 2015, pp. 851–858.

[15] J. Pratt, J. Carff, S. Drakunov, and A. Goswami, "Capture point: A step toward humanoid push recovery," in *Proceedings of 2006 IEEE-RAS International Conference on Humanoid Robots*, 2006, pp. 200–207.

[16] T. Koolen, T. de Boer, J. Rebula, A. Goswami, and J. Pratt, "Capturability-based analysis and control of legged locomotion, part 1: Theory and application to three simple gait models," *The International Journal of Robotics Research*, vol. 31, no. 9, pp. 1094–1113, 2012.

[17] B. J. van Hofslot, R. Griffin, S. Bertrand, and J. Pratt, "Balancing using vertical center-of-mass motion: A 2-d analysis from model to robot," *IEEE Robotics and Automation Letters*, vol. 4, no. 4, pp. 3247–3254, 2019.

[18] M. Vukobratović and J. Stepanenko, "On the stability of anthropomorphic systems," *Mathematical Biosciences*, vol. 15, no. 1, pp. 1–37, 1972.

[19] P. Sardain and G. Bessonnet, "Forces acting on a biped robot. center of pressure-zero moment point," *IEEE Transactions on Systems, Man, and Cybernetics - Part A: Systems and Humans*, vol. 34, no. 5, pp. 630–637, 2004.

[20] M. B. Popovic, A. Goswami, and H. Herr, "Ground reference points in legged locomotion: Definitions, biological trajectories and control implications," *The International Journal of Robotics Research*, vol. 24, no. 12, pp. 1013–1032, 2005.

[21] S. Kagami, K. Nishiwaki, T. Kitagawa, T. Sugihara, M. Inaba, and H. Inoue, "A fast generation method of a dynamically stable humanoid robot trajectory with enhanced ZMP constraint," in *Proceedings of 2000 IEEE-RAS International Conference on Humanoid Robots*, 2000.

[22] T. Sugihara, Y. Nakamura, and H. Inoue, "Real-time humanoid motion generation through ZMP manipulation based on inverted pendulum control," in *Proceedings of 2002 IEEE International Conference on Robotics and Automation*, vol. 2, 2002, pp. 1404–1409.

[23] S. Caron, Q. Pham, and Y. Nakamura, "ZMP support areas for multi-contact mobility under frictional constraints," *IEEE Transactions on Robotics*, vol. 33, no. 1, pp. 67–80, 2017.

[24] J. Englsberger, C. Ott, and A. Albu-Schäffer, "Three-dimensional bipedal walking control based on divergent component of motion," *IEEE Transactions on Robotics*, vol. 31, no. 2, pp. 355–368, 2015.

[25] T. Sugihara, K. Imanishi, T. Yamamoto, and S. Caron, "3D biped locomotion control including seamless transition between walking and running via 3D ZMP manipulation," in *Proceedings of 2021 IEEE International Conference on Robotics and Automation*, 2021, pp. 6258–6263.

[26] K. Mitobe, G. Capi, and Y. Nasu, "Control of walking robots based on manipulation of the zero moment point," *Robotica*, vol. 18, no. 6, pp. 651–657, 2000.

[27] A. Goswami, "Postural stability of biped robots and the foot-rotation indicator (FRI) point," *The International Journal of Robotics Research*, vol. 18, no. 6, pp. 523–533, 1999.

[28] S. Kajita, F. Kanehiro, K. Kaneko, K. Fujiwara, K. Harada, K. Yokoi, and H. Hirukawa, "Biped walking pattern generation by using preview control of zero-moment point," in *Proceedings of 2003 IEEE International Conference on Robotics and Automation*, vol. 2, 2003, pp. 1620–1626.

[29] T. Takenaka, T. Matsumoto, and T. Yoshiike, "Real time motion generation and control for biped robot -1st report: Walking gait pattern generation-," in *Proceedings of 2009 IEEE/RSJ International Conference on Intelligent Robots and Systems*, 2009, pp. 1084–1091.

[30] R. B. McGhee and A. A. Frank, "On the stability properties of quadruped creeping gaits," *Mathematical Biosciences*, vol. 3, pp. 331–351, 1968.

[31] T. Sugihara, "Standing stabilizability and stepping maneuver in planar bipedalism based on the best COM-ZMP regulator," in *Proceedings of 2009 IEEE International Conference on Robotics and Automation*, 2009, pp. 1966–1971.